Numerical Methods in Civil Engineering

Effect of Fling-Step on Seismic Response of Steel Eccentrically Braced Frame Structures

Bahram Rezayibana [*], Saeed Norozikalehsar [**], and Babak Nourollahi[***]

ARTICLE INFO

Article history:
Received:
October2017.
Revised:
December 2017.
Accepted:
January 2018.

Keywords:
Fling- Step, Near-Fault Earthquake, Eccentrically Braced Frame, Story Drift-Ratio, Displacement

Abstract:

Fling-step and forward directivity are two important characteristics of near-field earthquakes. Forward directivity occurs when the rupture propagates toward the site and arises in fault-normal direction for strike-slip faults. Fling-step is the consequence of permanent ground displacement imposed by near-field earthquakes and arises in strike-slip faults in the strike parallel direction. Fling-step effect produces permanent displacement at the end the culmination of displacement time history. This effect is usually omitted from the main record using the standard processing methods and therefore, cannot be determined for different structures. Many studies were performed to obtain seismic response of different structures subjected to near-field earthquake having forward directivity. On the other hand, there are few references to investigate the effect of fling-step on seismic behavior of structures. For this purpose, 14 earthquake records with fling-step are selected in a way that important factors including fling-step, PGV, PGA and the energy application type are different. The selected records are applied to eccentrically braced frame structures with 3, 6, 9 and 12 stories. A nonlinear time history analysis is used to capture displacement and story-drift ratio responses. The results show that the fling-step effect has no significant impact on any of the considered structures and its effect can be neglected in the case of eccentrically braced frame structures.

1. Introduction

Directivity and fling-step are two important characteristics of near-field earthquakes. Directivity is related to direction of rupture propagation and its effect is significant in the fault normal direction. Fling-step is induced by the permanent static displacement of the ground that is noticeable in strike-slip faults [1]. Fling-step is observed at the end of the record as a long period pulse in non-zero velocity and displacement records. These effects are usually neglected using the standard processing methods (Baseline correction, high-pass filter) for the strong ground motions [2]. The processed and unprocessed acceleration, velocity and displacement records in the north-south direction of the Darfield-New Zealand earthquake (2010) are shown in figure 1. Time histories obtained by the standard processing from the PEER net site [3] and the original time histories possessing fling-step are shown by the solid and dashed lines, respectively. It should be mentioned that the original time histories are obtained by the method proposed by Burks and Baker [4].

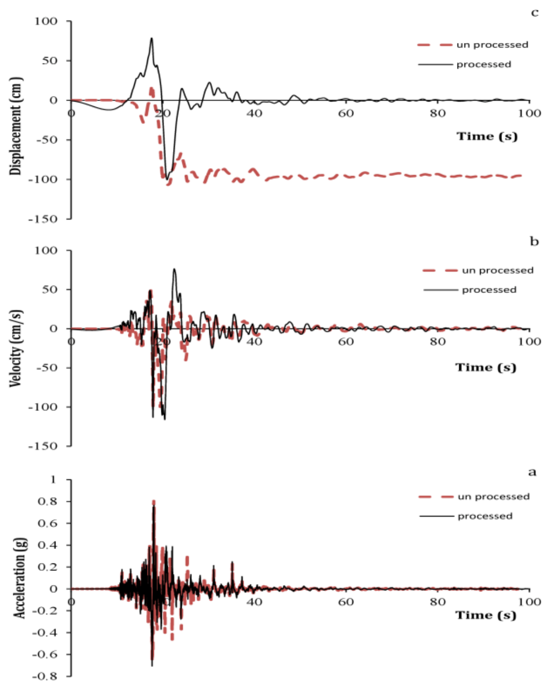

Fig. 1: Processed and unprocessed time histories of Darfield-New Zealand earthquake

[*] Corresponding Author: Assistant Professor, Department of Civil Engineering, Ardabil Branch, Islamic Azad University, Ardabil, Iran, Email: Bahram.deprem@gmail.com.

[**] Department of Civil Engineering, Tabriz Branch, Islamic Azad University, Tabriz. Iran.

[***] Department of Civil Engineering, Tabriz Branch, Islamic Azad University, Tabriz, Iran,

Filtering consists of applying a low- and high-pass filter to the frequency domain, which typically removes the fling-step effect from records [5]. Since the amplitude of the fling-step is highly sensitive to the choice of baseline, and baseline correction has a negligible effect on elastic response spectra, records are typically filtered and added to an engineering database [6]. Previous studies showed that structural response due to near field earthquakes is more severe than that of far-field records, and significantly depends on the pulse period to structure period [7-10]. There are only a few studies on the effect of near-field earthquakes with the fling-step effect. Stewart et al. (2001) obtained the structural response of the filtered records with added stochastic displacement pulses [11]. However, since this method omits the effects of standard processing, it cannot provide the desirable results [12]. Kalkan and Kunnath (2006) analyzed different structures under far-field and near-field earthquakes with directivity and fling-step effects [13]. They showed that, near-field earthquakes with fling-step characteristic were likely to make the structures more vulnerable compared to far-field earthquakes. Burks and Baker (2014) evaluated the single-degree-of-freedom systems using near-field earthquakes with different displacement characteristics. This included records with static offsets preserved via standard processing, records that were made by adding stochastic displacements to the filtered records, and records whose permanent displacement were omitted using a standard processing method [14]. They showed that, in most of the cases in single-degree-of-freedom systems, the structural response did not depend on fling-step. However, more studies on multi-degree-of-freedom systems are required. In this paper, the following questions would be answered: does the fling affect the seismic response of multi-story buildings and does scaling of the near-field accelerograms with fling change the characteristics of ground motions? For this purpose, eccentrically braced frames (EBF) with 3, 6, 9 and 12 stories are evaluated in the current study. Fourteen records with a fling-step effect are selected in a way that they include different seismic characteristics and the structural responses are obtained by nonlinear time history analysis using Sesimostruct software [15].

2. Details of the studied buildings

Four buildings with 3, 6, 9 and 12 stories are selected for the current study and EBFs with short link are used to design. Each structure has 5 spans in x and y directions. The span length in both directions is 5 meters and the story height is 3.2 meters. The lateral load resisting system of the buildings is eccentric braces with the link length equal to 60 cm. The column bases are assumed to be pinned to the foundation. The P-Δ effect is considered for the columns. The applied dead and live load on story floors is 6 KN/m2 and 2 KN/m2 respectively. The sections used for beams and columns are wide flange sections with a yield stress of 345 MPa. Braces are HSS section with a yield stress of 320 MPa. All structures selected in the region possess very high seismicity and soil type C (shear wave velocity between 366 and 762 m/sec) according to ASCE/SEI-7 (2010) [16]. The seismic load is determined according to ASCE/SEI-7. The plan of the structure is shown in figure 2.

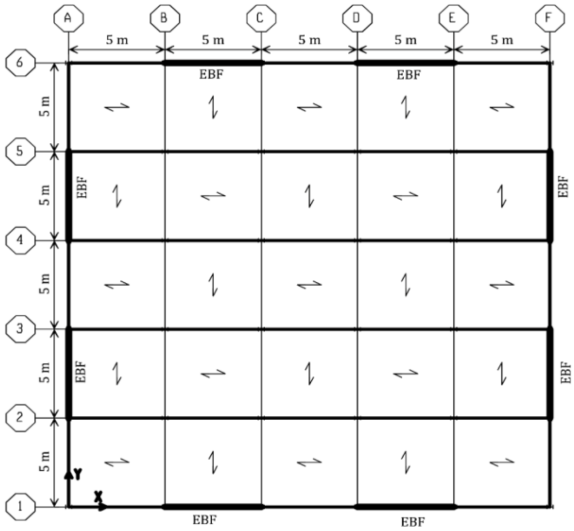

Fig. 2: Typical floor plan of buildings

One of the braced frames selected for conducting nonlinear time history analysis is designed according to AISC (2010) [17]. The elevation of 3, 6, 9 and 12-story frames are shown in Figures 3, 4, 5 and 6 respectively.

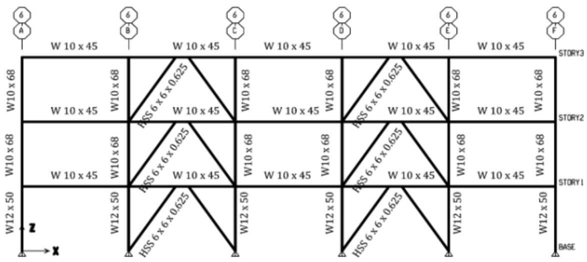

Fig. 3: EBF elevations of the 3-story building

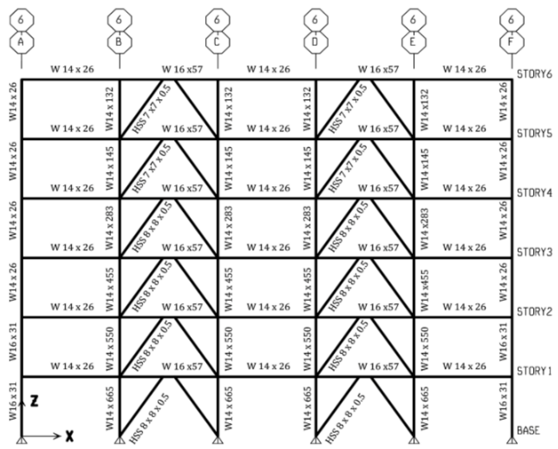

Fig. 4: EBF elevations of the 6-story building

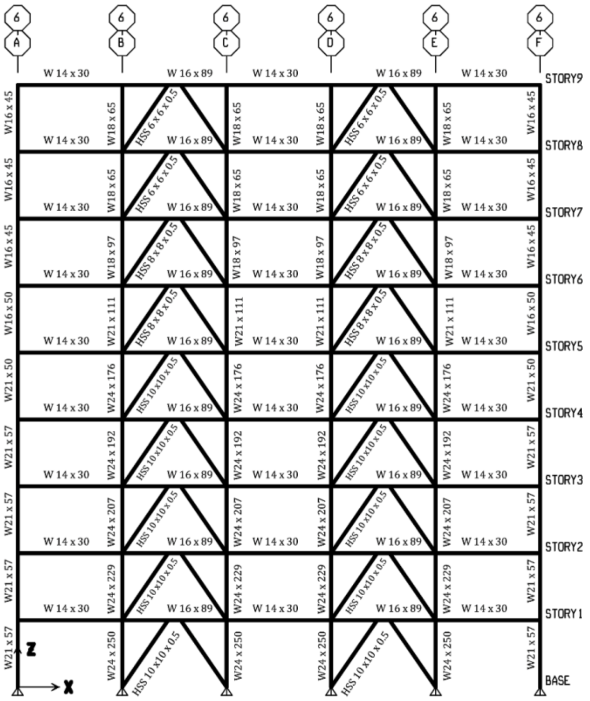

Fig. 5: EBF elevations of the 9-story building

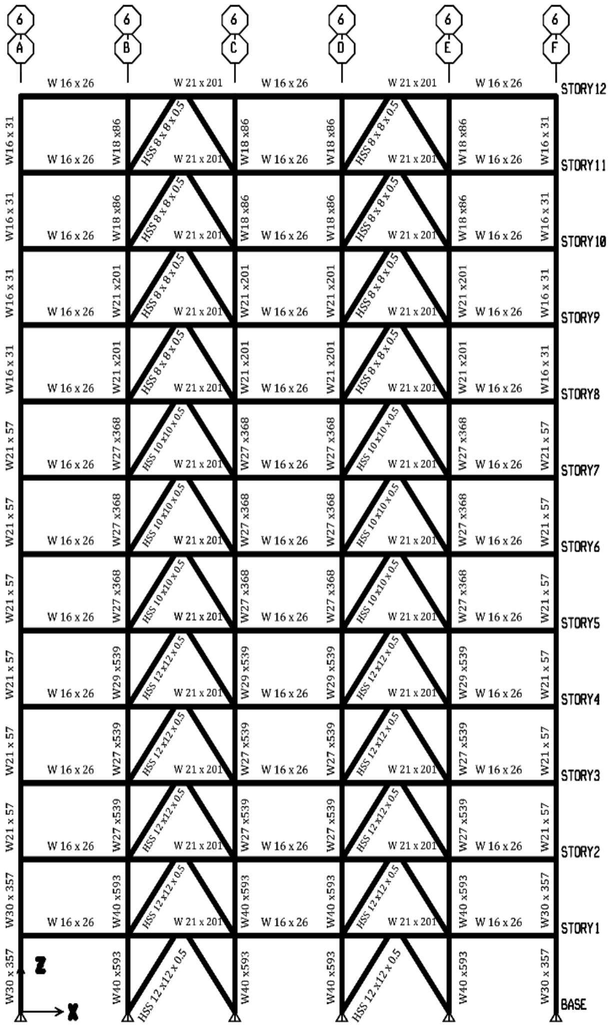

Fig. 6: EBF elevations of the 12-story building

3. Modeling of Braced Frames

Seismostruct software is used to design the models. This software is a common advanced finite element analysis tool, which is capable of simulating 3D and 2D frames by considering geometrical nonlinearity as well as inelastic material behavior under static and dynamic loads. The graphical environment of the software makes it possible to accurately model the structure and define material behavior and view the analysis results. It is capable of simulating various materials with different properties. In this study, all steel frames are made of Menegotto-Pinto material with isotropic and kinematic hardening with a strain hardening ratio of 1% [18]. To model the section of structural member elements (link beam, out of link beam, column and braces), nonlinear beam-column element of fiber section type with 150 fibers is used. Since the beam-to-column connections in EBF's are pinned, the link element with zero length is used to simulate the connection. The bending stiffness is assumed to be negligible for this element to make it a complete pin. To provide shear behavior of the link beam, two link elements with zero length are placed at the ends of the link beam using symmetric bilinear curve (ideal elasto-plastic symmetric behavior with a 1% strain hardening). The initial stiffness ($\mathrm{k_0}$) and the yield force ($\mathrm{V_y}$) are determined by the following equations [19].

$$K_0 = \frac{\mathrm{GA_w}}{\mathrm{e}} \tag{1}$$

$$V_y = 0.55 A_w d F_y \tag{2}$$

$$G = \frac{E}{2(1+\vartheta)} \tag{3}$$

In the above equations, $\mathrm{A_w}$is the area of link web section, e is the length of link beam, d is the section height of link, $F_y$is the nominal yield stress of link beam and ϑ is steel Poisson's ratio equal to 0.3. The numerical model of braced frame is shown in figure 7.

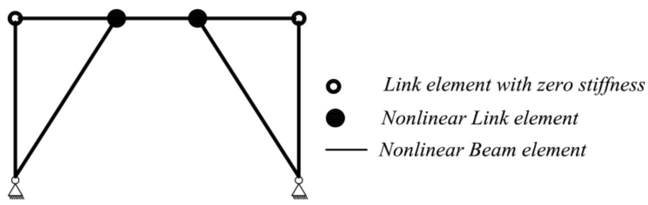

Fig. 7: Numerical model of EBF

Since the time history analyses are carried out in 2D space, the frames are modeled on the x-z plane. To limit the displacement of beam and column along the vertical direction to frame plane, displacement along the y direction and rotations on the x and z axes are fixed for beam-to-column joints. Beam-to-column connection and column-tobase connection are pinned. To conduct a dynamic analysis, mass should be assigned. Since four braced frames exist in each story and each frame has two columns, the story mass is divided by 8 and is applied to the beam-to-column joints as concentrated mass. To consider the structure damping, Rayleigh damping with 5% damping is used. To verify the numerical model, results of UT3A specimen in the experimental tests carried out by Mansour (2010) is used [20]. Details of the frame and loading are shown in figure 8.

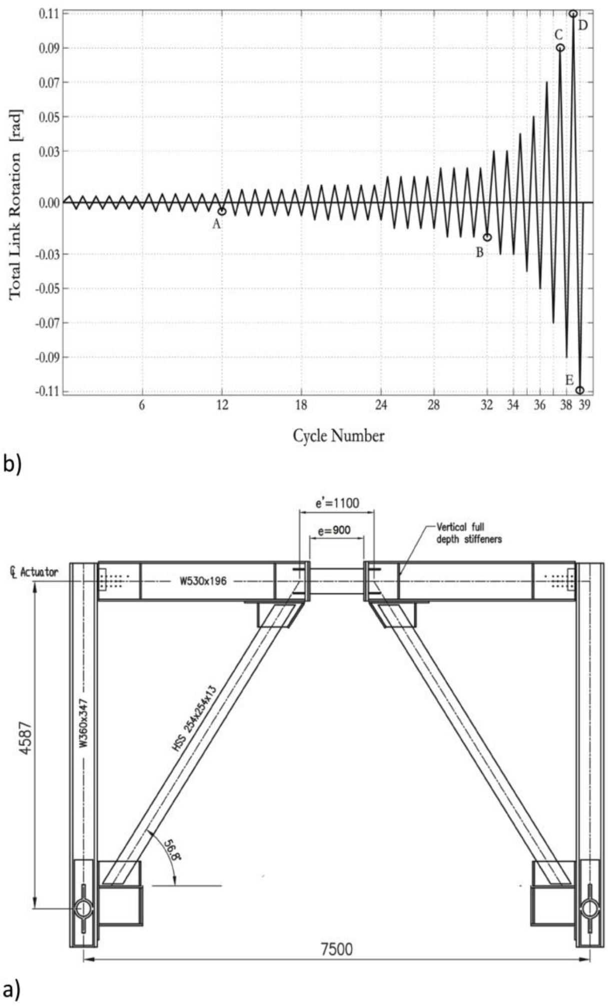

Fig. 8: a) Details of UT3A specimen [20], b) loading protocol of UT3A specimen [20]

As pointed out in the modeling section, the tested frame is modeled by the software. All boundary conditions are defined as in the test. Lateral cyclic loading is applied to the numerical model by converting link beam rotation to lateral displacement. The results of numerical analysis and the experimental test are shown in figure 9. As it can be seen, the numerical model can predict the real behavior of the frame with proper accuracy.

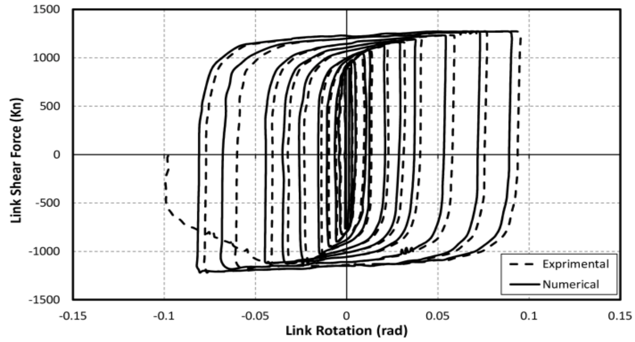

Fig. 9: Comparison of hysteresis response of numerical and experimental results

4. Ground Motion Database

In order to overcome the existing errors, the initial accelerograms recorded by accelerometers should be processed by using filtering and baseline correction (Standard Processing). In most of the cases, a small shift of the baseline results in an unreal linear increase in velocity and an unreal quadratic increase of displacement. To prepare the records for seismic investigation, these errors are corrected using standard processing. Since near-field earthquakes with a fling-step effect have permanent displacement at the end of the record, standard processing omits this displacement and the main record is basically changed with the elimination of fling-step. Many important world databases including the Pacific Earthquake Engineering Research (PEER 2016), Center for Engineering Strong Motion Data (CESMD 2012) [21] and the European Strong Motion Database [22] provide data of occurred earthquakes, while the fling-step effect is omitted from near-field earthquake records. However, Burks (2014) extracted 88 records with permanent displacement that could be used in seismic investigations [23]. These records are all obtained for soil type C and, thus, can be used for seismic evaluation of the designed structures. For the current study, 14 records out of the mentioned 88 are selected in a way that they can cover a wide range of frequency content, time duration, amplitude of acceleration, velocity and displacement records and the energy application rate. In the record selection, an attempt is made not to consider records with a velocity pulse to evaluate the effect of permanent displacement. The 14 selected records are presented in Table 1. In this table, the records are classified into two categories. Category A includes 8 records whose PGA and fling are different and PGV is approximately constant, such that the effect of energy application rate is omitted. Category B includes 6 other records. In this category, the records are selected in a way that the energy application rate is different. The records are classified into three cases; gradually, partially fast and fast, based on the energy application rate. The differences between the energy application rates are shown in figure 10. In the records called “gradually”, energy is gradually applied. In the records called “fast”, a greater amount of energy is applied within a short time. In the records called “partially fast”, some of the energy is applied fast and the rest is applied gradually.

Table 1. Ground motion database

No	NGA	Earthquake Name	Year	Station Name	Magnitude	Closest Dist. (km)	Direction	PGA (g)	PGV (cm/s)	Fling-disp (cm)	Energy applying rate	Vs30 (m/s)
Category A												
1	1497	Chi-Chi, Taiwan	1999	tcu057	7.6	11.83	EW	0.114	40.86	59.11	gradually	555
2	1521	Chi-Chi, Taiwan	1999	tcu089	7.6	0	NS	0.228	35.62	172	gradually	672
3	1532	Chi-Chi, Taiwan	1999	tcu105	7.6	17.16	NS	0.127	42.34	30	gradually	576
4	1551	Chi-Chi, Taiwan	1999	tcu138	7.6	9.78	EW	0.21	34	84	gradually	653
5	1488	Chi-Chi, Taiwan	1999	tcu048	7.6	13.53	EW	0.119	36.76	58.97	gradually	551
6	1499	Chi-Chi, Taiwan	1999	tcu060	7.6	8.51	EW	0.2	37.33	73.98	gradually	375
7	1534	Chi-Chi, Taiwan	1999	tcu107	7.6	16	EW	0.13	34.31	47	gradually	535
8	1553	Chi-Chi, Taiwan	1999	tcu141	7.6	24.19	NS	0.09	28	27	gradually	223
Category B												
1	1494	Chi-Chi, Taiwan	1999	tcu054	7.6	5.3	NS	0.196	46.04	114.04	gradually	461
2	1489	Chi-Chi, Taiwan	1999	tcu049	7.6	3.8	EW	0.247	59.48	72.02	gradually	487
3	1176	Kocaeli	1999	Yarimca (ypt)	7.51	1.38	NS	0.24	89	148	fast	297
8	1513	Chi-Chi, Taiwan	1999	tcu079	7.6	0	EW	0.43	34.39	133.13	gradually	364
5	1198	Chi-Chi, Taiwan	1999	chy029	7.62	10.96	NS	0.238	39.22	22.06	partially fast	545
6	1509	Chi-Chi, Taiwan	1999	tcu074	7.6	0	NS	0.379	48.74	136.68	partially fast	549

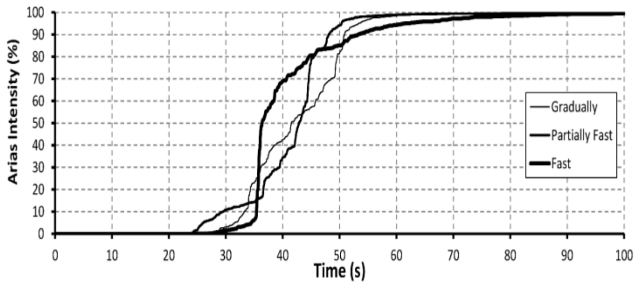

Fig. 10: Types of input energy of earthquake

5. Nonlinear time history analysis

By examining the 88 near-field records with the fling-step effect, it is concluded that their magnitudes are higher than 7, the distance from fault is less than 25 km and the soil type is C. Therefore, it can be said that the location of structures should be in an area with a very high seismic hazard containing very dense soil and soft rock. Considering the above assumptions, the designed structures are analyzed under the 14 selected records using nonlinear time history analysis and the responses are investigated. Moreover, to consider the effect of the response spectra and the effect of higher modes, the spectral values of acceleration and displacement for the first third modes of the designed structures are presented in Table 2.

5.1. Results of the 3-story structure

A comparison of displacement and story-drift ratio response for the 3-story structure under 14 selected earthquakes is shown in figure 11. As it can be seen from the average of the responses, the displacement variation along the structure height is approximately linear and it is related to the first vibration mode. The structure response of the tcu079 record is much higher than that of the other records due to the higher PGA and spectral values. The response of the 3-story structure in the two categories is shown separately in figure 12. In Category A, the maximum response is obtained for the tcu089 and tcu138 records and these responses are approximately the same.

Table 2. Ground motion database

	structures	3-Story			6-Story			9-Story			12-Story		
	Period (s)	1^{st} mode 0.44	2^{nd} mode 0.16	3^{rd} mode 0.10	1^{st} mode 0.70	2^{nd} mode 0.24	3^{rd} mode 0.14	1^{st} mode 1.23	2^{nd} mode 0.39	3^{rd} mode 0.20	1^{st} mode 1.45	2^{nd} mode 0.44	3^{rd} mode 0.22
records						Category A							
tcu057	Sa(g)	0.30	0.16	0.13	0.26	0.23	0.19	0.22	0.22	0.24	0.22	0.30	0.23
	Sd(cm)	1.45	0.10	0.03	3.16	0.330	0.09	8.11	0.78	0.24	11.47	1.45	0.27
tcu089	Sa(g)	0.55	0.72	0.44	0.34	1.08	0.58	0.30	0.64	0.59	0.26	0.55	0.81
	Sd(cm)	2.62	0.46	0.11	4.15	1.54	0.28	10.85	2.27	0.59	13.69	2.62	0.97
tcu105	Sa(g)	0.43	0.19	0.14	0.25	0.23	0.15	0.21	0.42	0.23	0.19	0.43	0.21
	Sd(cm)	2.07	0.12	0.04	3.00	0.32	0.07	7.83	1.51	0.23	9.62	2.07	0.25
tcu138	Sa(g)	0.58	0.38	0.32	0.34	0.47	0.42	0.23	0.63	0.42	0.22	0.58	0.40
	Sd(cm)	2.80	0.24	0.08	4.12	0.67	0.21	8.44	2.25	0.42	11.32	2.80	0.49
tcu048	Sa(g)	0.21	0.26	0.22	0.21	0.23	0.25	0.24	0.23	0.22	0.18	0.21	0.24
	Sd(cm)	0.98	0.16	0.05	2.56	0.32	0.12	8.92	0.81	0.21	9.16	0.983	0.28
tcu060	Sa(g)	0.37	0.35	0.24	0.34	0.42	0.32	0.24	0.47	0.35	0.17	0.37	0.46
	Sd(cm)	1.76	0.22	0.06	4.09	0.59	0.15	8.77	1.69	0.35	8.66	1.76	0.56
tcu107	Sa(g)	0.44	0.20	0.15	0.34	0.30	0.16	0.38	0.36	0.23	0.37	0.44	0.27
	Sd(cm)	2.12	0.12	0.04	4.17	0.43	0.08	13.87	1.28	0.23	19.01	2.12	0.33
tcu141	Sa(g)	0.16	0.14	0.10	0.14	0.15	0.13	0.14	0.16	0.16	0.20	0.16	0.15
	Sd(cm)	0.79	0.09	0.02	1.69	0.21	0.06	5.25	0.57	0.16	10.44	0.79	0.18
						Category B							
tcu054	Sa(g)	0.44	0.37	0.31	0.35	0.33	0.29	0.36	0.46	0.29	0.26	0.44	0.30
	Sd(cm)	2.08	0.23	0.08	4.24	0.48	0.14	13.31	1.65	0.29	14.28	2.08	0.35
tcu049	Sa(g)	0.53	0.69	0.33	0.51	0.74	0.56	0.34	0.55	0.63	0.24	0.53	0.54
	Sd(cm)	2.51	0.44	0.08	6.19	1.06	0.27	12.59	1.96	0.63	12.44	2.52	0.71
ypt	Sa(g)	0.68	0.53	0.33	0.73	0.59	0.45	0.44	0.55	0.46	0.28	0.68	0.49
	Sd(cm)	3.26	0.33	0.08	8.80	0.83	0.22	16.33	1.96	0.46	14.43	3.26	0.59
tcu079	Sa(g)	1.41	1.38	0.89	1.45	1.36	1.35	0.71	1.49	1.98	0.50	1.41	1.45
	Sd(cm)	6.74	0.88	0.22	17.54	1.95	0.65	26.20	5.33	1.96	25.60	6.74	1.74
chy029	Sa(g)	0.60	0.31	0.29	0.83	0.42	0.30	0.24	0.48	0.37	0.16	0.60	0.46
	Sd(cm)	2.86	0.20	0.07	10.01	0.60	0.15	8.66	1.72	0.37	8.13	2.86	0.55
tcu074	Sa(g)	0.75	0.79	0.63	1.33	0.61	0.80	0.52	0.95	0.77	0.55	0.75	0.74
	Sd(cm)	3.59	0.50	0.16	16.08	0.87	0.39	19.10	3.39	0.76	28.06	3.59	0.88

As it can be seen from Table 1, the PGA of these two records is the same, while the fling-step effect is higher in the tcu089 record than in tcu138. This shows that the fling-step effect on the responses is negligible. In the other 6 records, it is observed that when PGA increases, the response increases. A study of the spectral values shown in Table 2 shows that spectral values govern in the first period, and the higher spectral values in the first period result in the higher response of the 3-story structure under that record and the fling-step effect is negligible.

For Category B, the maximum response is obtained under the tcu079 record and the response is much different compared to the other responses. Since the spectral values of this record in the first mode is much higher than that of other 5 records, the response of 3-story structure is the maximum under this record. In the case of the other 5 records, the response is decreased when the spectral values in the first mode are reduced. It can be seen that, the spectral values and PGA are once more the most effective parameters whereas, the fling-step and the energy application rate barely affect the responses.

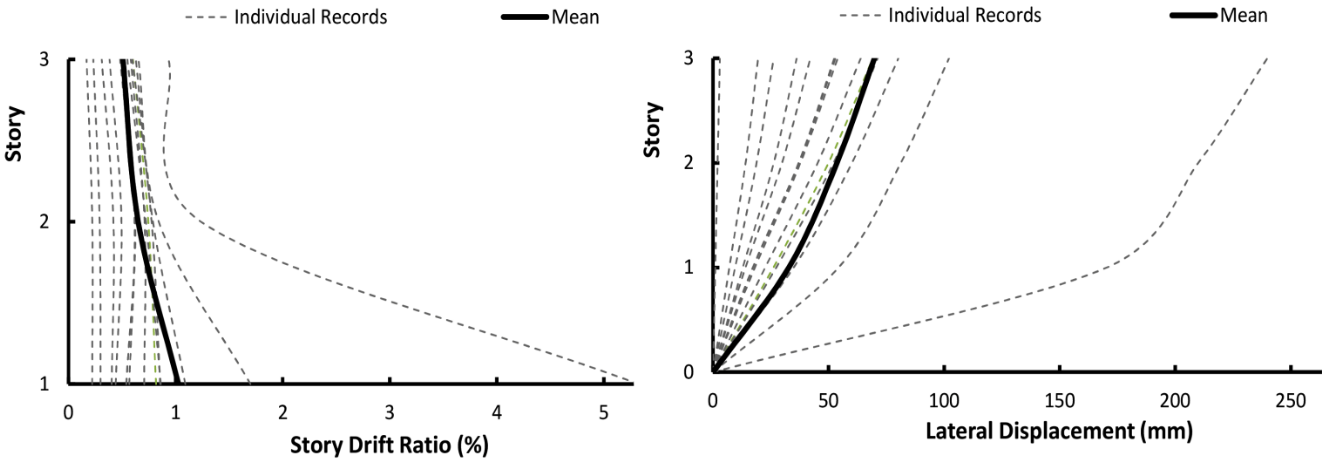

Fig. 11: Seismic response of the 3-story structure subjected to 14 selected records

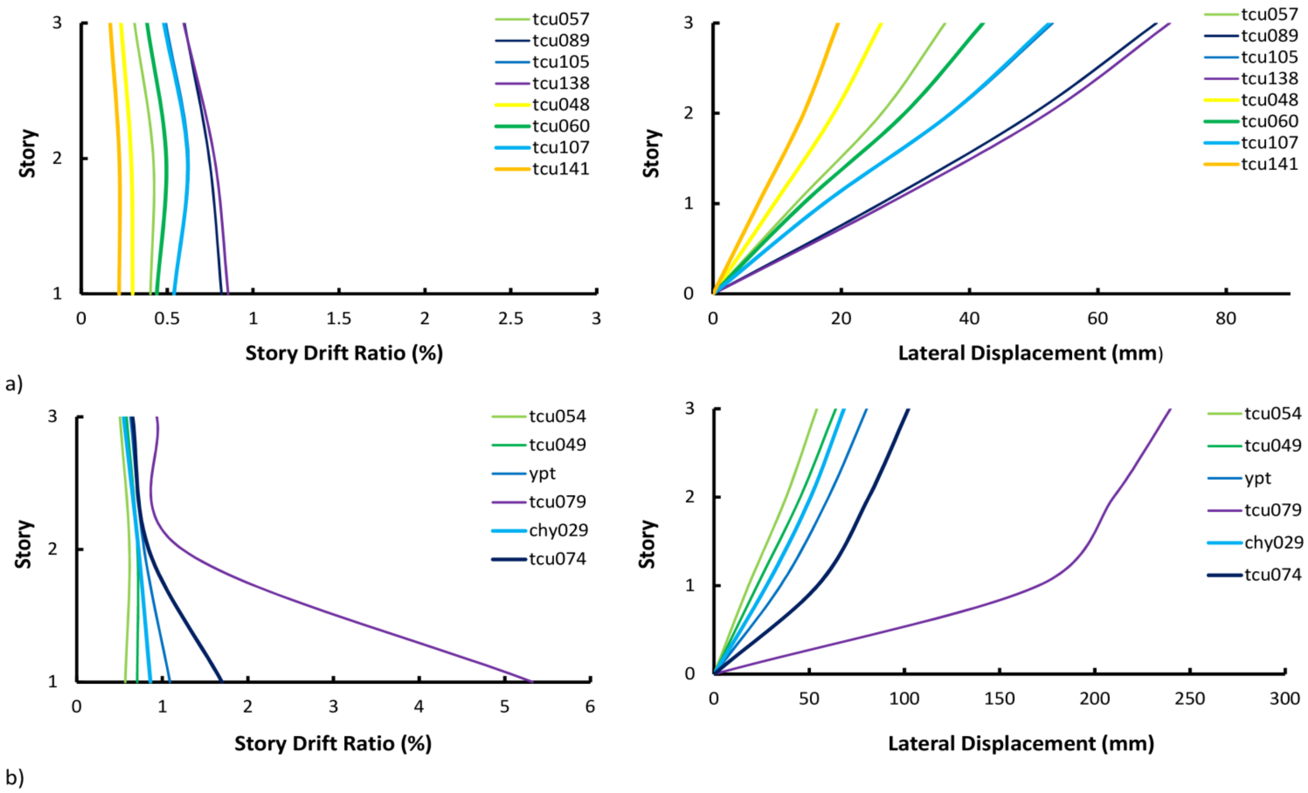

Fig. 12: Seismic response of the 3-story structure subjected to a) Category A and b) Category B

5.2. Results of the 6-story structure

The displacement and story-drift ratio response for the 6-story structure is shown in figure 13. As it can be seen, the response of the 6-story structure is approximately similar to the first mode. Although in some records, a small variance is observed, the average response of the 14 records is in good agreement with the first mode. The response of the 6-story structure is shown in figure 14 for Categories A and B separately. For Category A, the structure responses to the tcu060, tcu089, tcu107 and tcu138 records are higher. From Table 2, it is evident that, the acceleration spectra value for all four records in the first mode is approximately 0.34g and therefore, the displacement response of the 6-story structure to the four records is the same. Story-drift ratio response is rather different for the tcu089 record compared to that of the three other records. It is apparent that the story-drift ratio at higher stories under the tcu089 record is increased exhibiting the effect of higher modes. The spectral values of the tcu089 record for the second mode are much higher than that of the three other records, as displayed in Table 2, and consequently, the second mode has a specific participation.

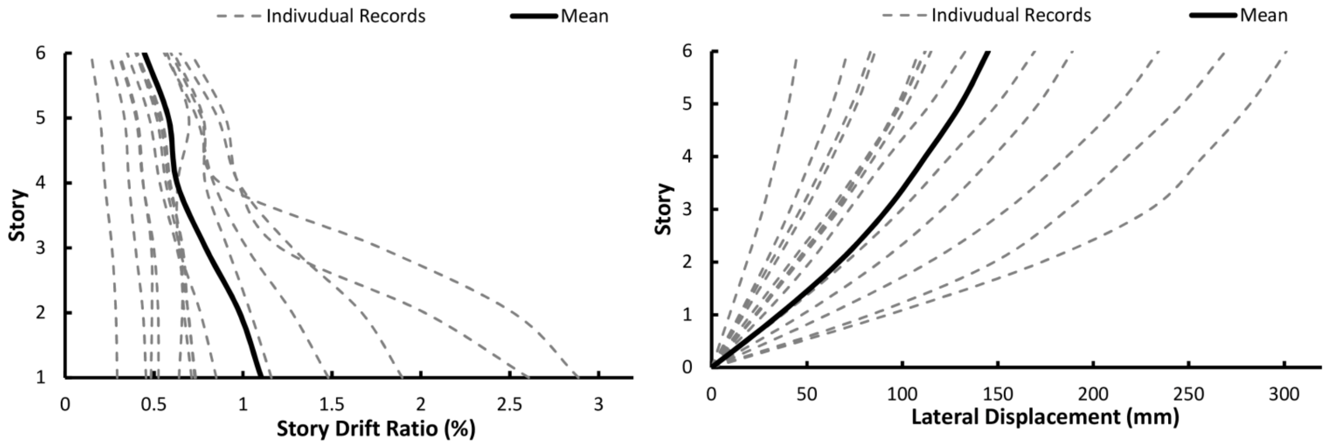

Fig. 13: Seismic response of the 6-story structure subjected to 14 selected records

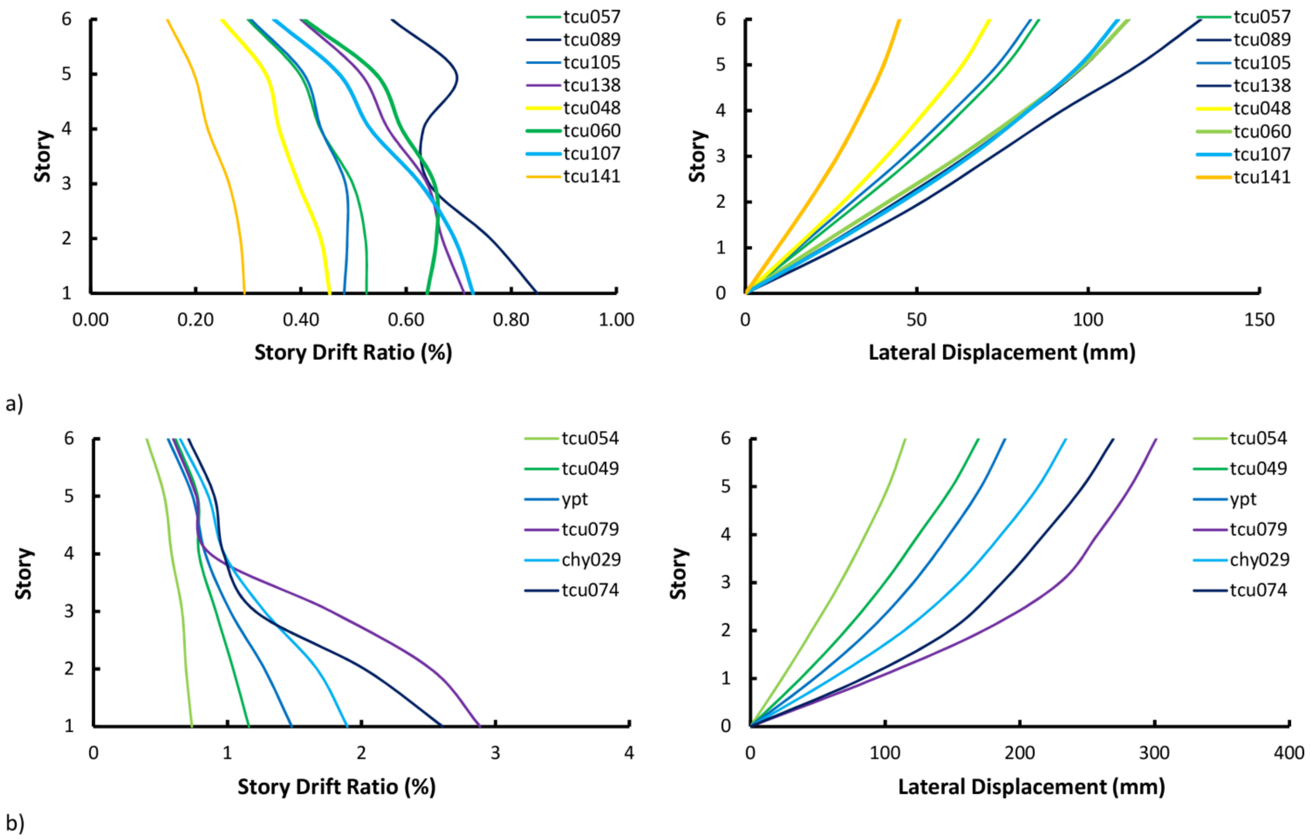

Fig. 14: Seismic response of the 6-story structure subjected to a) Category A and b) Category B

Comparison of responses under Category B shows that the displacement response to the tcu074 and tcu079 records is the maximum due to the high PGA and spectral values in the first mode. Although the energy application rate in these two records is lower than the chy029 record, the displacement response to the chy029 record is ranked third based on the amplitude value. By observing the story-drift response, the energy application rate has a significant effect on the responses at higher stories. When the energy application rate is increased, the response at the higher stories also increases. As it can be seen, the story-drift ratio values at higher stories is increased for the chy029 and tcu074 records that have higher energy application rate than that of the tcu079 record.

5.3. Results of the 9-story structure

A comparison of displacement and story-drift ratio response for the 9-story structure under the 14 selected records is shown in figure 15. It can be deduced from the average of the responses that the effect of higher modes is noticeable for some records. The response of the 9-story structure is shown in figure 16 for the Category A and B separately.

The results for Category A shows that, the response is the maximum for the tcu107 and tcu089 records and the responses are approximately the same for the tcu138, tcu105, tcu060, tcu057 and tcu048. This phenomenon was not observed in the 3- and 6- story structures. As depicted in Table 2, the spectral acceleration values are 0.29g and 0.38g for the tcu089 and tcu107 records respectively whereas, this value is 0.24g for the other five records. It is observed that the fling-step does not affect the responses. However, as it can be seen from story-drift ratio, this ratio is increased at upper stories to the applied records. The reason can be attributed to a higher spectral acceleration value in the second and third modes of these records showing that higher modes are activated. It is also observed that the fling-step has no significant effect.

The responses under Category B show that spectral values have the maximum effect, and the energy application rate is at the next rank. As it can be deduced from Table 2, the spectral acceleration value in the first mode for the ypt, tcu074 and tcu079 records are 0.443g, 0.520g and 0.713g respectively. This shows that the response will increase when spectral acceleration is increased. Although the chy029 record has a fast energy application rate, lower response is induced due to lower spectral values. Since the difference between spectral values in the first mode under the tcu079 and tcu074 records is great, energy application rate cannot have any effect on the responses, in contrast to the 6-story structure. In the majority of the records, spectral values in the second and the third modes are higher than that of the first mode and higher modes affect the response of the 9-story structure. As it was observed, the energy application rate and the fling-step do not affect the results.

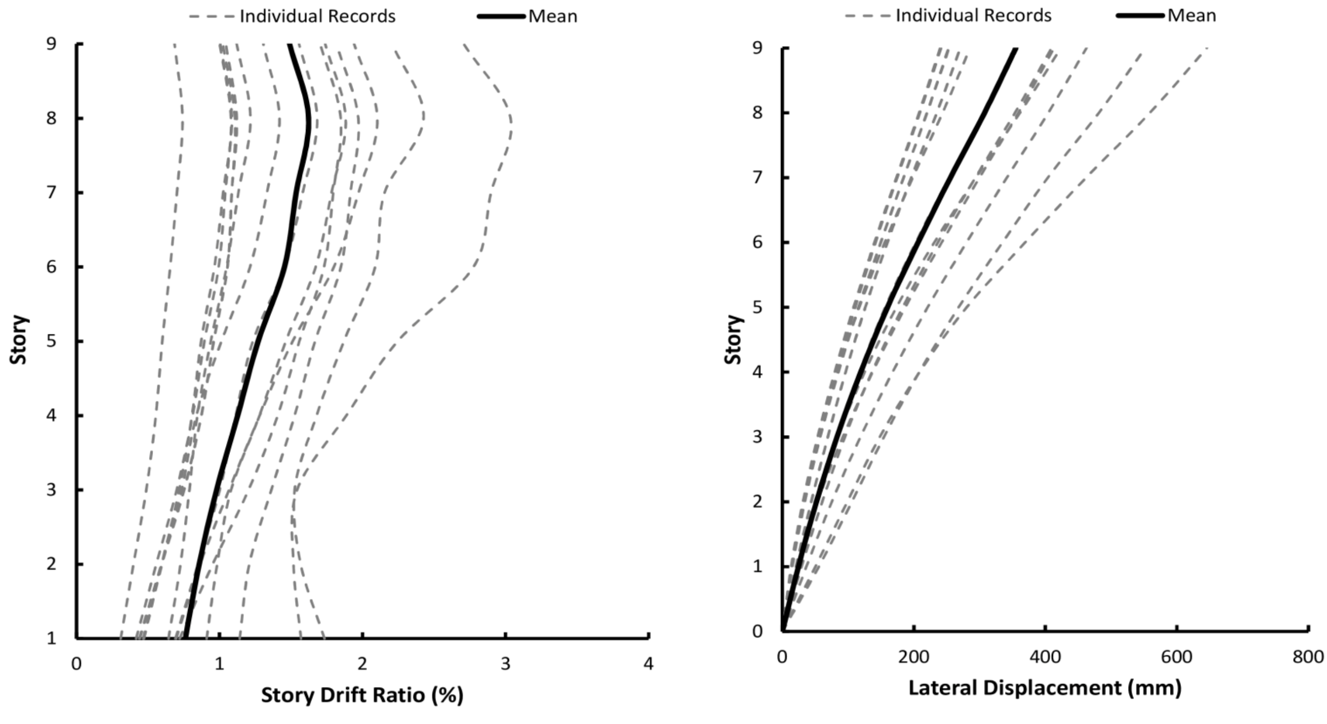

Fig. 15: Seismic response of the 9-story structure subjected to 14 selected records

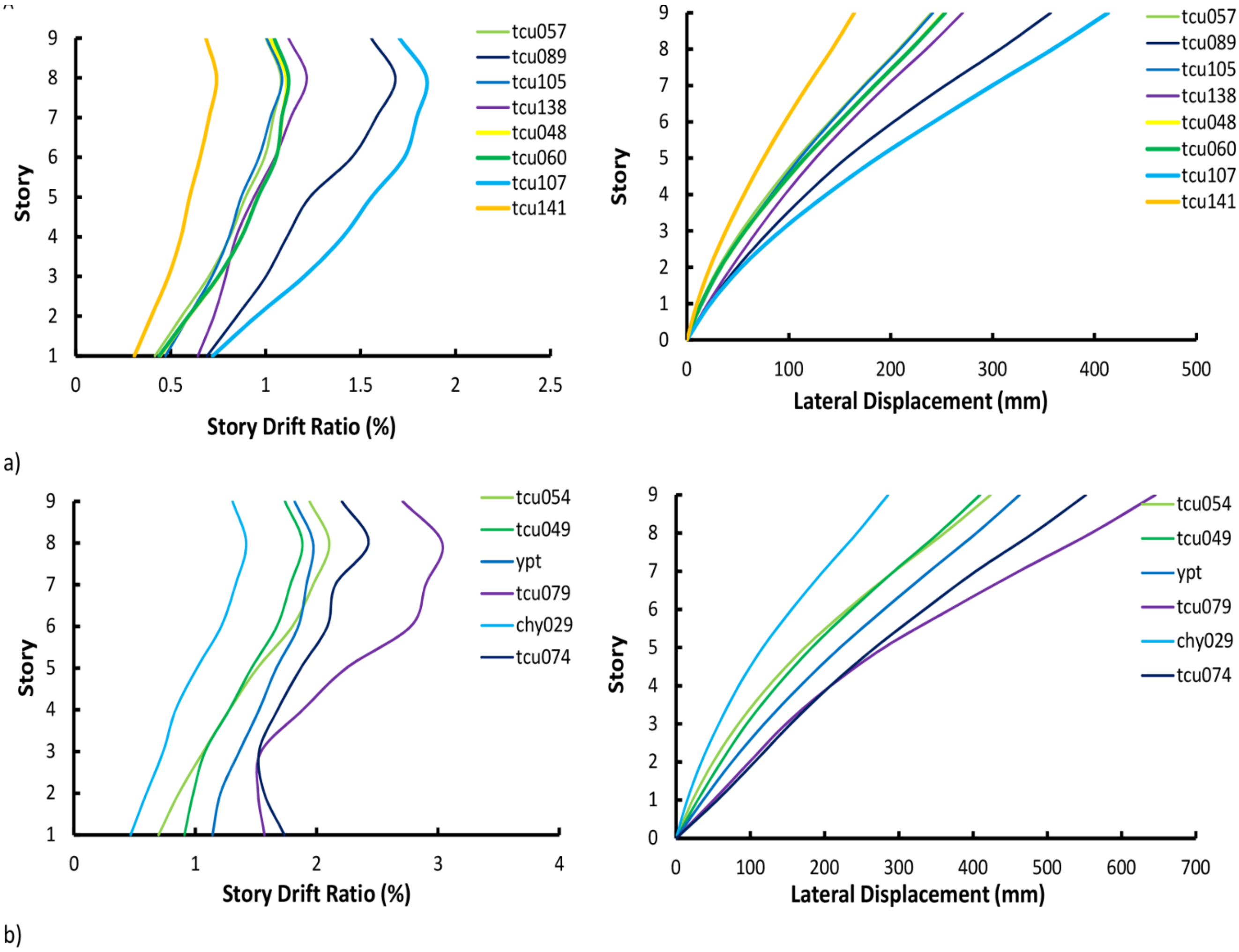

Fig. 16: Seismic response of the 9-story structure subjected to a) Category A and b) Category B

5.4. Results of the 12-story structure

A comparison of displacement and story-drift ratio response for the 12-story structure under the 14 selected records is shown in figure. 17. The average of the responses indicates that the displacement change along the height is almost in agreement with the first mode and the effect of the higher modes is not noticeable, except for the tcu074 and tcu079 records. The response of the 12-story structure under Category A and B is shown in figure 18.

The results for Category A show that the response under the tcu107 record is at the first rank, based on the maximum response, with a significant difference from the second rank, although the response is almost the same as that of the tcu089 record at lower stories. As shown in Table 2, the spectral acceleration values are larger under the tcu107 record compared to that of the tcu089 record resulting in the generation of the maximum response. Although the fling-step effect of the tcu089 record is much higher than that of the tcu107 record, it is again observed that the fling-step effect hardly has any effect. Furthermore, structure responses under other records are affected by spectral values.

The response of the 12-story structure under Category B shows that spectral values have the maximum effect and the energy application rate is at the next rank. As seen from shown in Table 2, the spectral acceleration value in the first mode for the tcu074 and tcu079 are 0.55g and 0.50g respectively. This shows that the response increases when the spectral acceleration is increased. Since the spectral values of these two records are close, the responses coincide. Therefore, when the difference of the spectral values is close, energy application rate cannot significantly affect the structure response. However, some differences that are induced at upper stories are shown in the It is apparent that the response under the chy029 record is lower than that of the other records. Although the energy application rate is the maximum in this record compared to that of the other records, the response decreases since the spectral values in the first mode are at the minimum compared to that of the other records.

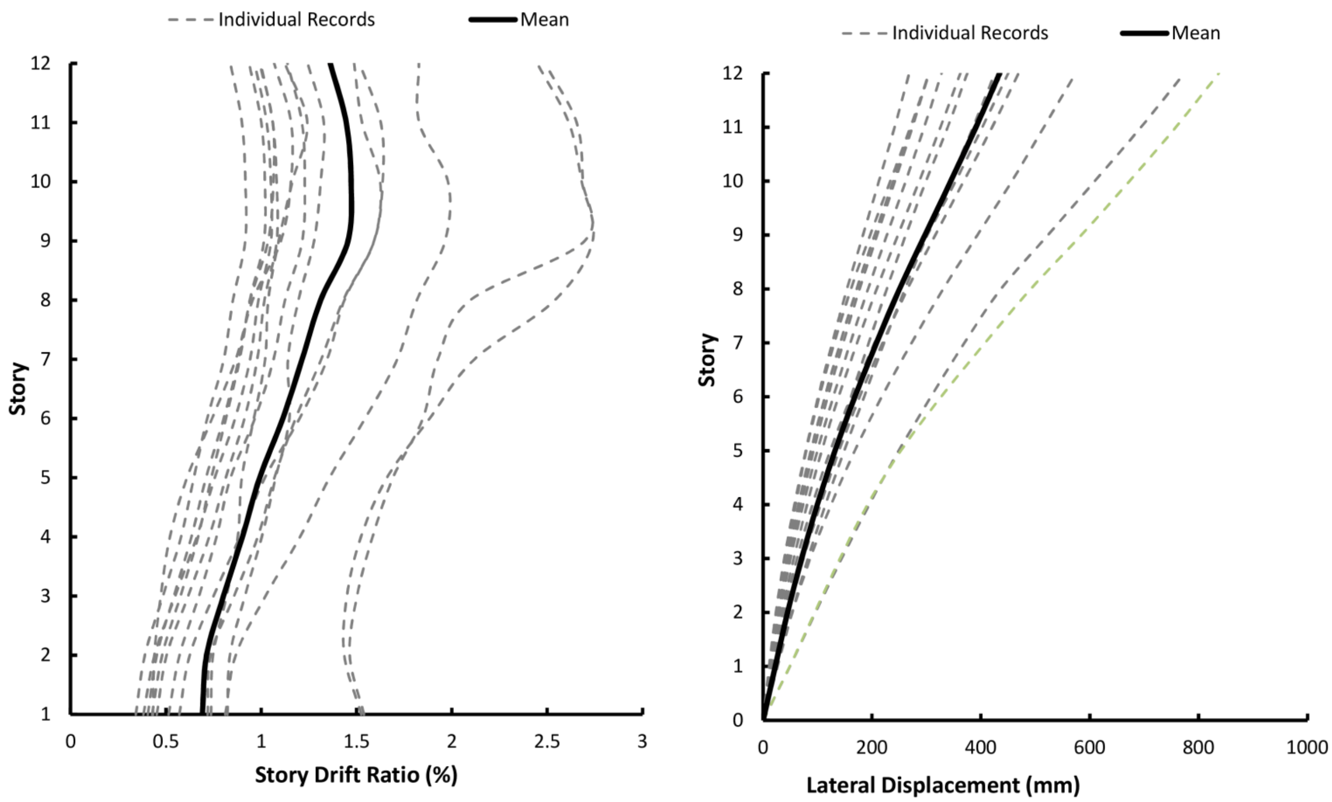

Fig. 17: Seismic response of the 12-story structure subjected to 14 selected records

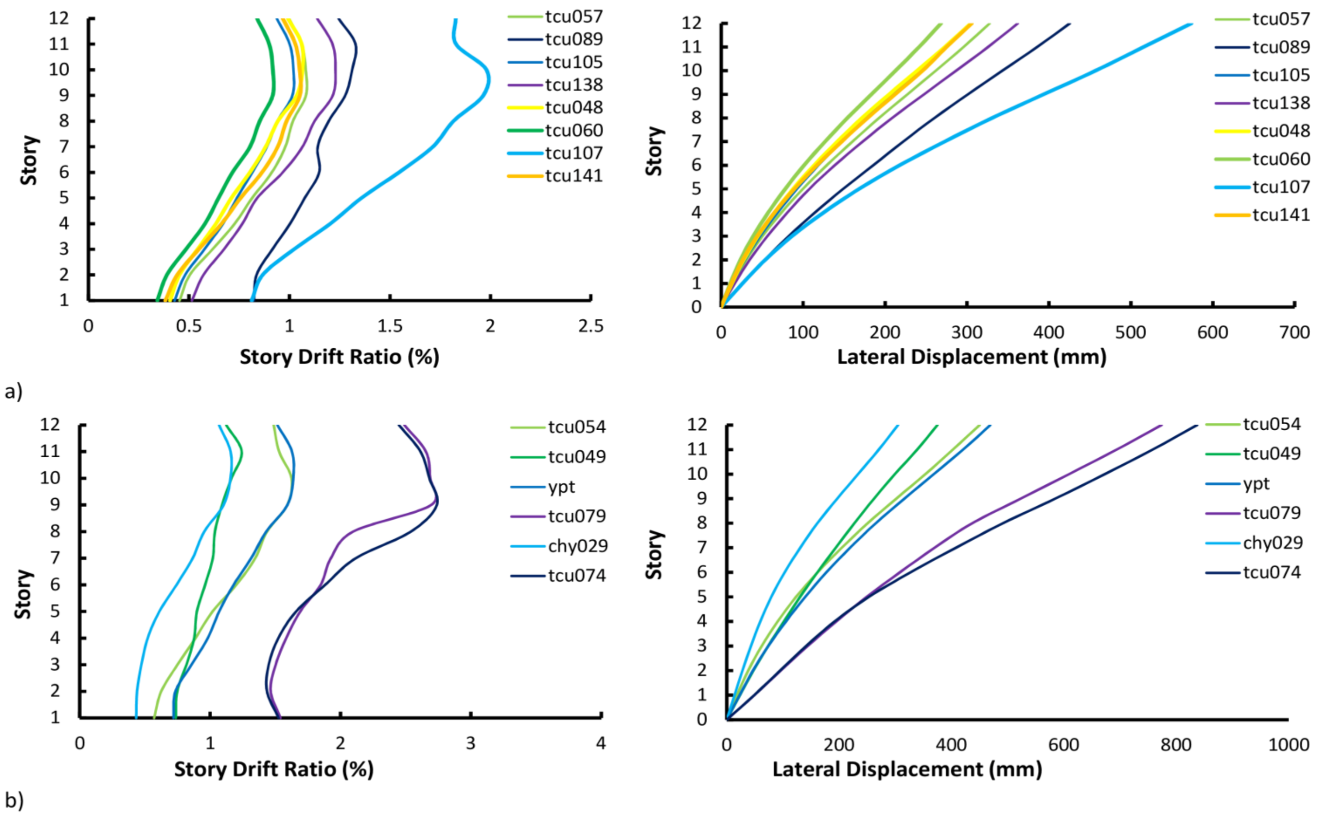

Fig. 18: Seismic response of the 12-story structure subjected to a) Category A and b) Category B

5.5. Comparison of the responses to filtered/unfiltered ground motions

The structures are re-analyzed under selected records with and without fling-step effects (filtered and unfiltered) to study the influence of fling-step on displacement responses. The tcu074, tcu079 and ypt records are selected, as they have the highest response to the frames. Figure 19 summarizes the displacement responses of 3, 6, 9 and 12-story structures to the three selected ground motions as filtered/unfiltered.

As shown in Fig. 19, the responses of the structures to the filtered and unfiltered are approximately the same. It is concluded that the fling-step does not have any effect on the response of the structures and can be omitted from the records as shown in the previous section.

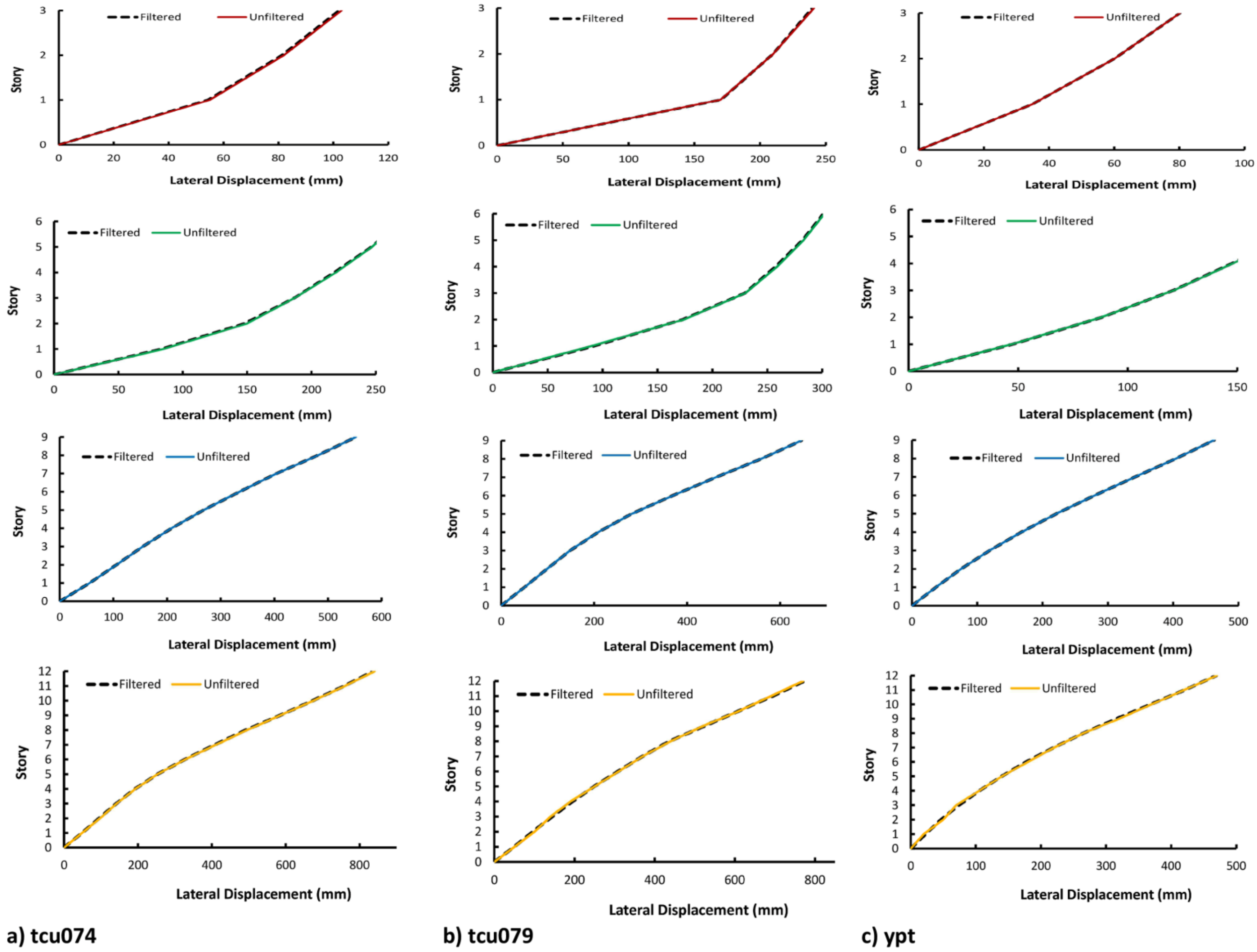

Fig. 19: Displacement response of the 3, 6, 9 and12-story structure subjected to filtered/unfiltered records

6. Conclusions

In this study, 4 structures with eccentric braces and different stories were designed according to AISC (2010). The designed structures were then exposed to 14 earthquake records with the fling-step effect and nonlinear time history analysis was carried out and the results were examined. The earthquake records were selected in a way that the parameters including fling-step, PGV, PGA, spectral values and energy application rates were different to make the study of the fling step effect as accurate as possible. The analysis results showed that in eccentrically braced frames with 3, 6, 9 and 12 stories, the fling-step did not have noticeable effect on the responses. The most effective parameter on displacement and story-drift ratio response is the spectral values for the first mode in the case of 3-story structures and the spectral values of the first and second modes in the case of 6, 9 and 12-story structures. Moreover, it is concluded that when the spectral values in the first mode are close, the energy application rate can affect the response at higher stories. When the spectral values are far, the energy application rate does not affect the responses even if a higher percentage of earthquake energy is applied to the structure within a short time. Generally, it is concluded that steel eccentrically braced frame structures are not sensitive to fling-step and its effect can be omitted from the records, as it is done in most of world databases using standard processing. Therefore, it can be said that sensitivity exists in scaling near-field earthquake records with directivity but does not exist in the case of near-field earthquakes with fling-step and they can be scaled and used in time history analysis.

References:

[1] Somerville, P.G., Smith, N. F., Graves, R.W. and Abrahamson, N. A. (1997). “Modification of Empirical Strong Ground Motion Attenuation Relations to Include the Amplitude and Duration Effects of Rupture Directivity”, Seismological Research Letters, Vol. 68, No.1, PP.199–222

[2] Boore, D. M. and Bommer, J. J. (2005). “Processing of strong-motion accelerograms: Needs, options and consequences”, Soil Dynamics and Earthquake Engineering, Vol. 25, PP. 93–115

[3] PEER ground motion database (2016). Available at http://peer.berkeley.edu/peer_ground_motion_database

[4] Burks, L.S. and Baker, J.W. (2016). “A predictive model for fling-step in near-fault ground motions based on recordings and simulations”, Soil Dynamics and Earthquake Engineering, Vol. 80, PP.119-126

[5] Kamai, R., Abrahamson, N. and Graves, R. (2014). “Adding fling effects to processed ground- motion time histories”, Bulletin of the Seismological Society of America, Vol. 104, No. 4, PP. 1914–1929

[6] Kamai, R. and Abrahamson, N. (2015). “Are near-fault fling effects captured in the new NGA West2 ground motion models”, Earthquake Spectra, Vol. 31, No. 3, PP. 1629-1645

[7] Alavi, B. and Krawinkler, H. (2001). “Effects of near-fault ground motions on frame structures,” Blume Earthquake Engineering Center Technical Report 138, Stanford, CA

[8] Zhang, Y. and Iwan, W.D. (2002). “Active interaction control of tall buildings subjected to near-field ground motions”, Journal of Structural Engineering ASCE, Vol. 128, No. 1, PP. 69–79

[9] Calugaru, V. and Panagiotou, M. (2012). “Response of tall cantilever wall buildings to strong pulse type seismic excitation”, Earthquake Engineering and Structural Dynamics, Vol. 41, No. 9, PP. 1301–1318

[10] Yahyai, B., Rezayibana, B. and Mohammadrezapour, E. (2011). “Effect of near-fault earthquakes with forward directivity on telecommunication towers”, Earthquake Engineering and Engineering Vibration, Vol. 10, PP. 211-218

[11] Stewart, J. P., Chiou, S. J., Bray, J. D., Graves, R. W., Somerville, P. G. and Abrahamson, N. A. (2001). “Ground Motion Evaluation Procedures for Performance-Based Design”, Pacific Earthquake Engineering Research Center Technical Report 2001/09, Berkeley, CA

[12] Ventura, C. E., Archila, M., Bebamzadeh, A. and Liam Finn, W. D. (2011). “Large coseismic displacements and tall buildings”, Structural Design of Tall and Special Buildings, Vol. 20, PP. 85–99

[13] Kalkan, E. and Kunnath, S. K. (2006). “Effects of Fling Step and Forward Directivity on Seismic Response of Buildings”, Earthquake Spectra, Vol. 22, No. 2, PP. 367–390

[14] Burks, L. S. and Baker, J. W. (2014). “Fling in near-fault ground motions and its effect on structural collapse capacity”, Tenth U.S. National Conference on Earthquake Engineering Frontiers of Earthquake Engineering July 21-25, Anchorage, Alaska 10NCEE

[15] SeismoStruct (2016) .A computer program for static and dynamic nonlinear analysis of framed structures. SeismoSoft, Ltd, Available from: www.seismosoft.com

[16] ASCE7-10 (2010). Minimum design loads for buildings and other structures, American Society of Civil Engineers, Reston

[17] AISC. (2010). Seismic provisions for structural steel buildings, American Institute of Steel Constructions, Chicago

[18] Yahyai, B. and Rezayibana, B. (2015). “Direct displacement-based design of special concentrically-braced frames in near-fault regions”, Bulletin of Earthquake Engineering, Vol. 13, PP.2945–2971

[19] Welleman. (2006). Shear Stiffness of Cross section, Springer, ISBN 987-1-4020-4123-5

[20] Mansour, N. (2010). “Development of The Design of Eccentrically Braced Frames with Replaceable Shear Links”, Ph.D. thesis, Civil Engineering Department., University of Toronto

[21] CESMD. (2012). Center for engineering strong motion data, Available at www.strong motioncenter.org

[22] Ambraseys, N. N., Smit, P., Douglas, J., Margaris, B., Sigbjornsson, R., Olafsson, S., Suhadolc, P. and Costa, G. (2004). “Internet site for European strong-motion data”, Bollettino di Geofisica Terorica e Applicata, Vol. 45, No. 3, PP.113–29

[23] Burks, L. S. (2014). “Ground motion simulations: Validation and application for civil engineering problems”, Ph.D. thesis, Stanford, CA, Stanford University